Philippine Engineering Journal (2002) XXIII (1): 59-76

Parametric and Kinetic Study of Silicon Nitride Film Deposition on Silicon Wafer by Low Pressure Chemical Vapor Deposition (LPCVD) Method

Angelito A. Velasco
Instructor
Department of Mining, Metallurgy and Materials Engineering
College of Engineering
University of the Philippines

ABSTRACT

Silicon nitride films were deposited on silicon wafers by Low-Pressure Chemical Vapor Deposition (LPCVD) method. Reaction gases were ammonia and 20% silane in nitrogen. The effects of (A) deposition temperature, (B) chamber pressure , (C) NH_3-SiH_4 flowrate ratio and (D) deposition time on the thickness of the film produced were studied using a full 2^k factorial design. The film thickness was found to increase proportionally with temperature, pressure and time, and inversely with NH_3-SiH_4 flowrate ratio. Analysis of variance (ANOVA) shows that all main effects and interactions AC, AD, and CD were statistically significant at 99% confidence level. An interactive first order model was fitted to the experimental data:

$$Y = 158.46 + 70.39X_1 + 26.86X_2 - 66.44X_3 + 74.45X_4 - 29.3X_1X_3 + 33.35X_1X_4 - 30.68X_3X_4$$

A kinetic study was also conducted in order to determine the rate equation for the growth of silicon nitride on silicon. The computed activation energy was 21.454 kcal/mol, which indicates that the surface reaction is rate limiting. The rate equation was:

$$\text{Deposition rate, nm/min} = 37661.7 \exp(-4578.5/T).$$

Scanning electron micrographs show that the silicon nitride deposits appear as spherical-cap shaped clusters. Energy dispersive x-ray (EDX) and x-ray diffraction (XRD) analyses confirm the formation of silicon nitride.

I. Introduction

1.1 Properties and uses of silicon nitride

Silicon nitride is an important dielectric material in device fabrication. Silicon nitride film possesses good masking properties with respect to ions of different metals especially sodium, and is used as a passivating layer in integrated circuits to protect the device from corrosion. It is an excellent diffusion mask for gallium, aluminum and zinc, with which SiO_2 reacts. Silicon nitride is used as the dielectric in dynamic random access memory (DRAM) capacitors, and in thin

film transistors (TFT's)[1,2]. It is also widely used as membrane material in micromachined sensors and actuators[3,4]. At high temperatures silicon nitride oxidizes very slowly and prevents the oxidation of the underlying silicon, making it a suitable masking material in the local oxidation of silicon (LOCOS) process. Silicon nitride films have the capability of remembering and retaining charges of both signs for a long time, and are used in nonvolatile memory devices. Silicon nitride promises to be a viable gate dielectric in place of silicon dioxide as IC devices continue to shrink in dimensions, and as anti-reflection coating on commercial crystalline solar cells[5, 6].

1.2 Low Pressure Chemical Vapor Deposition

Chemical vapor deposition (CVD) is a method of synthesizing materials by the chemical reaction of the components of the vapor phases near or on the substrate surface to form a solid film[7]. The process consists of passing carrier gases into a heated chamber under controlled conditions. At elevated temperatures, these gases decompose and react to form the solid film on the substrate placed inside the chamber. Low pressure CVD became of industrial importance as a method of material synthesis starting from the middle of the 70's. Prior to this time, chemical vapor deposition was done under atmospheric conditions. LPCVD reactors are typically operated at a pressure ranging from 0.1 to 1 torr. The reduction in pressure results to an increase in the diffusivity of the gas species by a factor of 1000. This facilitates transfer of the process from a *mass-transport-limited* to a *surface-reaction-limited* one. With hot wall LPCVD reactors, fairly uniform temperature distribution can be achieved, thus the deposition uniformity tends to be excellent. Deposition rates are lower for low pressure systems, however, since LPCVD reactors are not constrained by mass transport, wafers can be stacked vertically at close spacing thereby increasing wafer throughput[8,9]. Figure 1 shows a schematic of the LPCVD reactor.

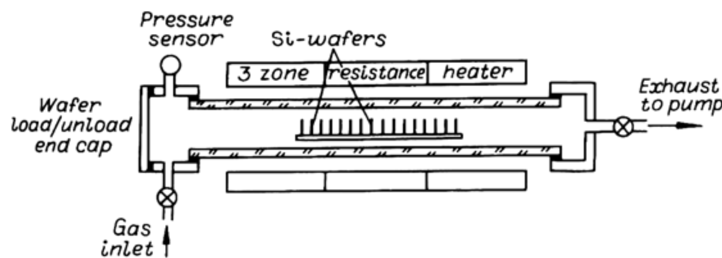

Figure 1. Schematic view of the LPCVD reactor (After Belyi[10]).

1.3 Significance of the study

The fabrication of integrated circuit (IC) devices has not yet been realized in the Philippines. Technological improvement in this field may prove to be very crucial in sustaining our county's economic growth. Equipped with *layering and patterning* apparatus, the U.P. Mining, Metallurgical and Materials Engineering (U.P.MMME) Department, made fabrication of semiconductor devices a major research thrust. This study is part of the DOST-PCASTRD funded project entitled "Development of Patterning and Layering Procedures for Semiconductor Device Fabrication". The objectives of this study are the following: (1) to determine the effects of the deposition parameters on the thickness of silicon nitride; and (2) to characterize the deposited film. The results generated from this research will enhance the local data bank and enable the fabrication of simple devices in the future.

II. Methodology

2.1 Experimental Set-Up

Figure 2 shows the schematic of the LPCVD set-up. The reaction chamber was a high purity silica tube with an internal diameter of 4.125 cm., thickness of 0.45 cm., and length of 55 cm. This tube was inserted into a 30 cm. long tube furnace. A rotary vane pump was used to evacuate the chamber to a base pressure of 0.015 torr. The reaction gases used were 20% SiH_4 in N_2 and NH_3. N_2 gas was used to purge the reaction chamber and to dilute the exhaust gases.

Figure 2. Schematic diagram of the LPCVD set-up

2.2 Sample Preparation

The substrates were prepared by cutting the silicon wafer into 1 x 1 inch dimension followed by cleaning using a method developed by the Radio Corporation of America (RCA). The solutions used in the RCA method are given in Table 1.

Table 1
Solutions used in the RCA cleaning method.

Solution	Composition	Ratio	Purpose
RCA 1	H_2O:H_2O_2:NH_4OH	4:1:1	Removal of residual organic contaminants and certain metals
RCA 2	H_2O:H_2O_2:HCl	4:1:1	Desorption of remaining atomic and ionic contaminants
RCA 3	H_2O:HF	4:1	Stripping of thin anhydrous oxide film

2.3 Film Deposition

The deposition chamber made of high purity quartz was placed into the tube furnace and connected to the gas lines. The silicon wafers were placed into the wafer holder and inserted into the chamber. The chamber was then evacuated by switching on the rotary vane pump. To flush out air, nitrogen gas was introduced into the reaction chamber for about 3 minutes. Evacuation of the chamber followed until the chamber pressure reached 0.015 torr. The furnace temperature was then set to the designed deposition temperature. When the desired temperature was attained, the reaction gases were introduced into the chamber according to their designed flow rates. Final adjustment of the chamber pressure was accomplished by introducing nitrogen gas through a leak valve located between the chamber and the rotary vane pump. When the desired time of deposition has been reached, the supply of reaction gases was cut off and the temperature of the furnace reduced. Nitrogen purge was done to ensure the complete removal from the chamber of the silane and ammonia gases. The wafers were removed from the chamber and stored for analysis.

2.4 Film Characterization

To determine the film thickness, a Nanospec AFT model# 10-180 Ellipsometer was used. This instrument has an accuracy of ±5 nm. In Ellipsometry, a polarized light is shone on to a sample surface at an oblique angle of incidence. The polarization of light reflected parallel and perpendicular to the sample surface is measured. This allows the relative phase change and relative amplitude change from the reflected surface to be determined. The intensity of the monochromatic reflected light depends strongly on film thickness because of interference. Given the refractive index of the film, its thickness can be determined according to Hamilton[11] using the equation:

$$x_o = \frac{\lambda}{2n_i}\left[g - \left(\phi_s - \phi_f\right)\right] \quad (1)$$

where x_o is film thickness, λ is the wavelength (in vacuum) of the incident radiation, ϕ_s is the relative phase shift at the film/substrate interface, ϕ_f is the relative phase shift at the air/film interface, n_i is the index of refraction of the film, and g is the order of the interference[12].

Scanning electron microscopy (SEM) was used to study the surface morphology of the deposited films. To determine the film composition, energy dispersive x-ray (EDX) and x-ray diffraction (XRD) analyses were employed.

III. Results and Discussion

3.1 Parametric study

3.1.1 Result of factorial experiment for film thickness response

A full 2^k factorial experimental design with replicated centerpoint runs was used in this study. Table 2 shows the different settings used for the factors considered.

Table 2
Factor Settings

Setting	A Temp, °C	B Pressure, Torr	C NH3-SiH4 ratio	D Time, min
Low(-)	800	4	33	20
High(+)	900	6	99	60
Centerpoint	850	5	66	40

The average film thickness data from the factorial experiment is given in the second and fourth columns of Table 3. Measurements of the film thickness were made with an ellipsometer using a refraction index of 2.01. Five thickness readings at various points near the center of each sample surface were taken and averaged. The thinnest film was obtained for treatment combination (c) with a value of 19.32 nm and the thickest film was obtained for run (abd) measuring 555.32 nm. Table 4 shows the analysis of variance (ANOVA) table for the factorial runs.

From the ANOVA table, the main effects of all the factors investigated were found to be significant 99% confidence level. Also found significant at 99% confidence level were the two-factor interaction effects between (1) deposition temperature and NH_3/SiH_4 flowrate ratio (AC), (2) deposition temperature and deposition time (AD), and (3) NH_3/SiH_4 flowrate ratio and deposition time (CD). No three or four factor interaction effects were found to be significant.

Table 3

Experimental response from the 2^k factorial experiment

Treatment combination	**Average film thickness nm**	**Treatment combination**	**Average film thickness nm**
1	56.56	bd	220.44
a	150.44	abd	555.32
B	86.32	cd	56.5
ab	203.18	acd	180.32
c	19.32	bcd	102.22
ac	62.76	Abcd	221.52
bc	43.12	centerpoint	148.9
abc	85.22	centerpoint	123.5
d	154.92	centerpoint	141.0
ad	406.8	centerpoint	150.8

Table 4

Analysis of variance for film thickness response

Source of Variation	**Sum of Squares**	**Degrees of Freedom**	**Mean Square**	**Computed f**
A	79264.8	1	79264.8	513.1*
B	11541.2	1	11541.2	74.7*
C	70623.1	1	70623.1	457.2*
D	88672.9	1	88672.9	574.0*
AC	13738.2	1	13738.2	88.9*
AD	17795.6	1	17795.6	115.2*
CD	15057.7	1	15057.7	97.5*
Error	463.4	3	154.5	
Critical f (99%)	= 34.1			

Significant at 99% confidence level.

3.1.2 Main Factor Effects

Effect of Temperature on film thickness

A plot showing the effect of temperature on the silicon nitride film thickness is given in Figure 3. The points in the plot correspond to the average thickness of all factorial runs with low level, centerpoint, and high level settings of deposition temperature respectively. An increase in the deposition temperature from 800 to 900°C resulted to an increase in average film thickness of 141 nm from 92 to 233 nm. This is because higher deposition temperatures result to faster reaction rates. Consequently, more of the reaction products are formed resulting to a thicker deposit.

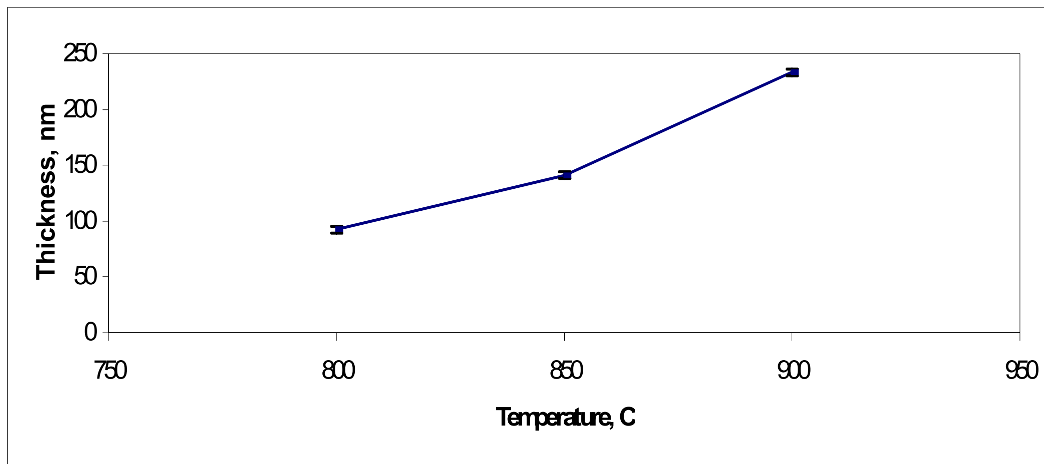

Figure 3 Plot of average film thickness versus deposition temperature.

Effect of chamber pressure on film thickness

Figure 4 shows a plot of the average film thickness versus the total pressure inside the deposition chamber. From the figure it can be seen that increasing the pressure from 4 to 6 torr increases the average film thickness from 136 to 190 nm, a difference of 54 nm. In this experiment, the chamber pressure was varied by changing the nitrogen gas flow. The rate of nucleation is directly proportional to the total pressure, therefore, increasing pressure results to an increase in thickness. Of the four factors considered, the chamber pressure had the lowest computed f value as shown in Table 4.

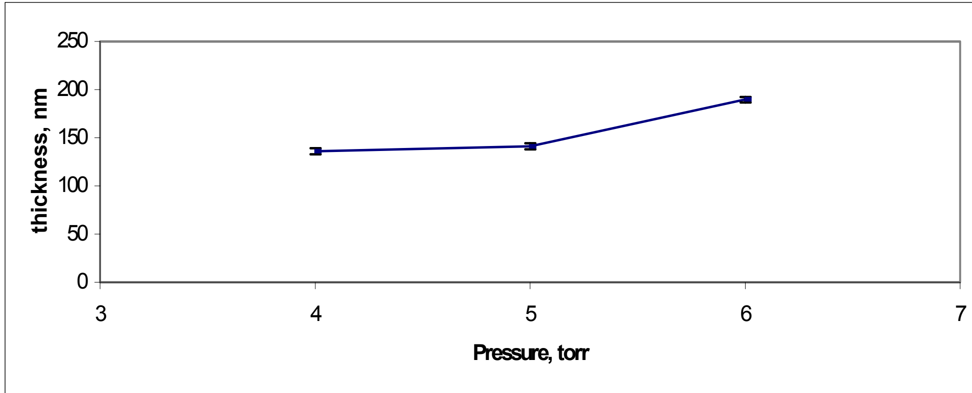

Figure 4 Plot of average film thickness versus chamber pressure.

Effect of NH_3/SiH_4 flowrate ratio on thickness

NH_3 gas was maintained at a flowrate of 99 sccm for all treatment combinations. The flowrate ratio was varied by changing the SiH_4 flowrate. Increasing the SiH_4 flowrate decreases the NH_3/SiH_4 flowrate ratio. The thickness of the silicon nitride film is greatly affected by the flowrate ratio of the reaction gases as can be seen in Figure 5. Increasing the NH_3/SiH_4 flowrate ratio from 33 to 99 decreases the average film thickness by 133 nm from 229 to 96 nm. The reason for this is that lower NH_3/SiH_4 ratio means more silane in the gas stream and correspondingly more silicon available to react with nitrogen to form the solid silicon nitride.

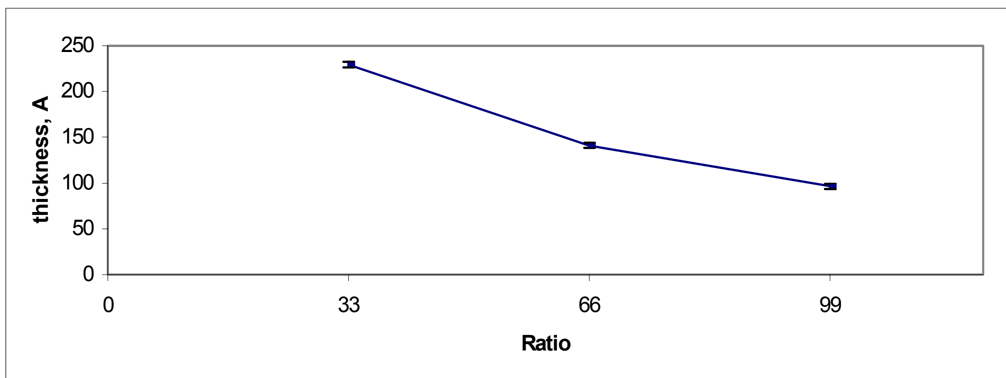

Figure 5 Plot of average film thickness versus NH_3-SiH_4 flowrate ratio.

Effect of deposition time on thickness

Figure 6 is a plot of the film thickness versus deposition time. Increasing the deposition time from 20 minutes to 60 minutes resulted to an increase in average film thickness by 149 nm from 88 to 237 nm. The effect of deposition

time gave the largest computed f value in the ANOVA table (Table 4). Longer deposition time means more collisions; therefore, more layers are incorporated into the film.

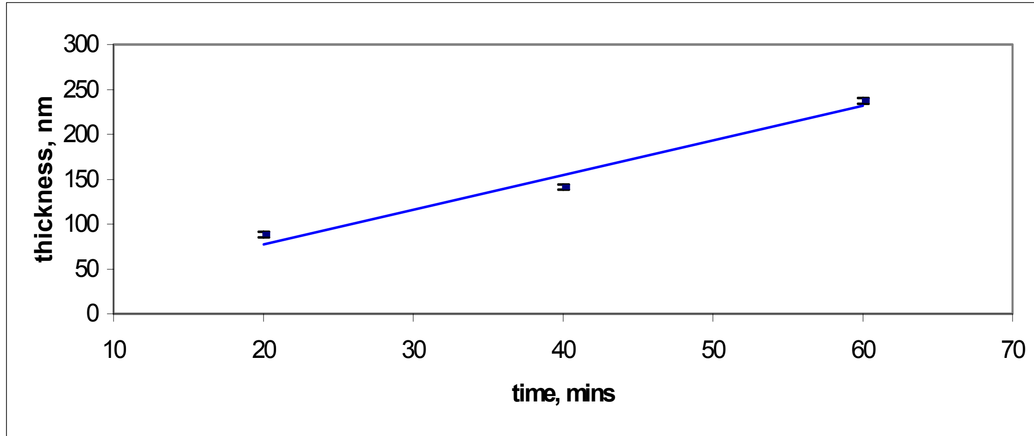

Figure 6 Plot of film thickness versus deposition time.

3.1.3 Parameters of the Interactive First-Order Model

The interactive first-order model to be fitted to the experimental data is given by the equation

$$Y = b_0 + b_1X_1 + b_2X_2 + b_3X_3 + b_4X_4 + b_{13}X_1X_3 + b_{14}X_1X_4 + b_{34}X_3X_4 \quad (2)$$

where Y = film thickness in nanometers

X_1 = deposition temperature, coded variable

= (temperature in °C - 850)/(50)

X_2 = chamber pressure, coded variable = (pressure in torr - 5)/1

X_3 = ammonia/silane flowrate ratio, coded variable = (ratio - 66)/33

X_4 = deposition time, coded variable = (time in minutes - 40)/20

b_0 = average response

b_1, b_2, b_3, b_4 = Effect of factors /2

b_{13}, b_{14}, b_{34} = interaction parameters = Effect of interactions/2

The parameters of the interactive first-order equation can be determined using appropriate procedures[13]. All the main and interaction effects of the factors considered which are significant at 99% confidence level were included in this model. Therefore, the interactive first-order prediction equation is

$$Y = 158.46 + 70.39X_1 + 26.86X_2 - 66.44X_3 + 74.45X_4 - 29.3X_1X_3 + 33.35X_1X_4 - 30.68X_3X_4 \quad (3)$$

Goodness of Fit Test

A plot of predicted versus experimental response is shown in Figure 7. From the analysis of variance table (Table 5) it can be concluded that the lack-of-fit error is not significant at 95% confidence level, since the computed f (7.48) is less than the critical f (8.81). The model therefore adequately fits the experimental data. The SSR/SST value of the model is quite high, being equal to 0.965. This means that the model accounts for 96.5% of the observed experimental variation.

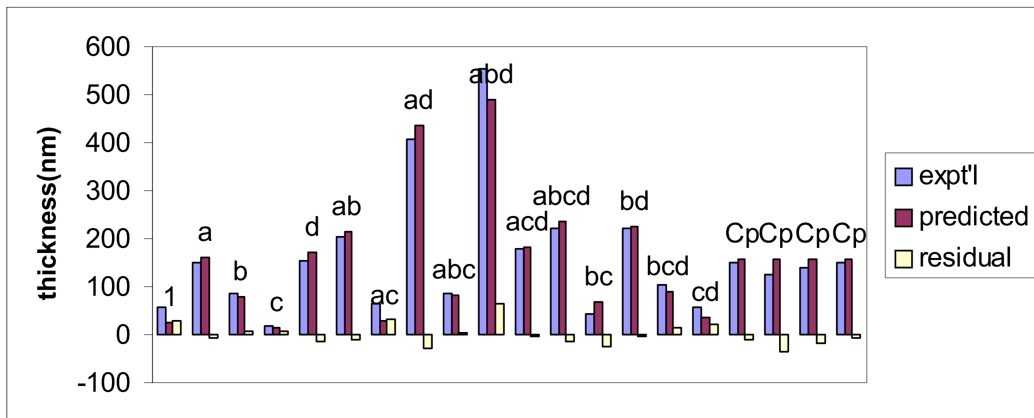

Figure 7 Plot of experimental response vs. predicted response.

Table 5

Analysis of variance table for the model.

Source of variation	SS	DOF	MS	Comp f	Critical f (95%)
Regression	296693.4	7	42384.8		
Total Error	10856.1	12	904.7		
lack of fit	10392.7	9	1154.74	7.48	8.81
pure	463.4	3	15448.01		
Total	307549.5	19			
SSR/SST	0.965				

3.1.4 Interaction Effects

Temperature and NH_3/SiH_4 flowrate ratio

Figure 8 shows the plot of the average film thickness vs. deposition temperature and NH_3/SiH_4 flowrate ratio. Film thickness is shown to increase with increase in temperature and decrease in NH_3/SiH_4 flowrate ratio. The unequal slopes of the lines in Figure 8 clearly show the interaction between deposition temperature and NH_3/SiH_4 flowrate ratio. The slope of the thickness vs. temperature line is steeper at lower NH_3/SiH_4 flowrate ratio. Decreasing the NH_3/SiH_4 flowrate ratio from 99 to 33 increases the effect of temperature on film thickness by 2.4 as computed by taking the ratio of the slopes.

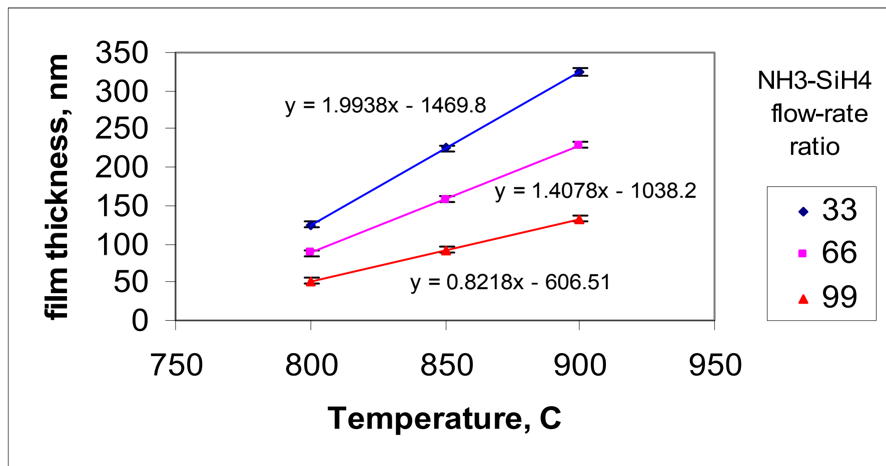

Figure 8 Plot of average film thickness vs. deposition temperature and NH_3/SiH_4 flowrate ratio. Chamber pressure = 5 torr, deposition time = 40 mins. *(Note: curves cannot be extrapolated to T =0 °C since silicon nitride films are deposited above 700 °C)*

Deposition time and NH_3/SiH_4 flowrate ratio

Figure 9 shows a plot of average film thickness vs. deposition time and NH_3/SiH_4 flowrate ratio. Film thickness is shown to increase with increase in deposition time and decrease in NH_3/SiH_4 flowrate ratio. Interaction between deposition time and NH_3/SiH_4 flowrate ratio is evident from Figure 9. Decreasing the NH_3/SiH_4 flowrate ratio from 99 to 33 increases the effect of time on thickness by 2.4.

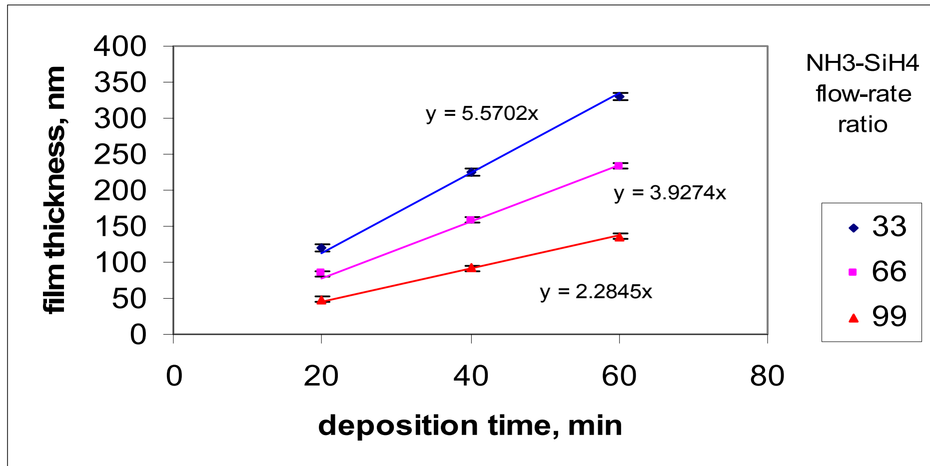

Figure 9 Plot of average film thickness vs. deposition time and NH_3-SiH_4 flowrate ratio. Temperature = 850 °C, chamber pressure = 5 torr.

3.1.5 Film thickness uniformity

Film thickness at various points on the wafer surface was recorded. The thickness gradient parallel to the reactor tube ranges from 5 to 10 nm per inch, and from 2 to 5 nm per inch perpendicular to it. This variation was due to the uneven temperature distribution within the chamber. Regions near the heating elements were thicker since the temperature in this region was higher.

3.2 Kinetic Study

In the kinetic study, the chamber pressure and the NH_3/SiH_4 flowrate ratio were maintained constant at 6 torr and 99 respectively. Figure 10 shows the plot of silicon nitride film thickness versus the deposition time at various deposition temperatures. It can be seen that the film thickness increases linearly with deposition time. For higher deposition temperatures, the slope becomes steeper. The rates of deposition, *k*, in nm/min were determined from the slope of the lines in Figure 10.

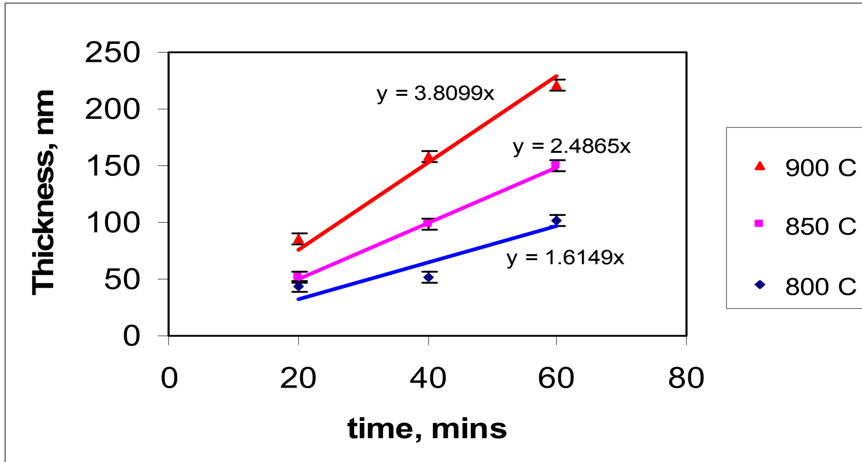

Figure 10 Plot of film thickness vs. deposition time. Pressure=6torr, NH_3-SiH_4 flowrate ratio =99

In logarithmic form, the Arrhenius' equation can be written as

$$\log k = \log A - \left(\frac{E_a}{2.3R}\right)\left(\frac{1}{T}\right) \tag{4}$$

where A is the Arrhenius constant, E_a is the activation energy in kcal/mol, R is the gas constant (= 1.98923 x 10^{-3} kcal/mol-K), and T is the absolute temperature in Kelvin (K). Plotting *log k* versus *1/T* gives us the Arrhenius' plot as shown in Figure 11. The activation energy, E_a, can be determined from the slope of the line which is equal to $-E_a/2.3R$. The Arrhenius' constant, A, can be determined from the *y-intercept* which is equal to *log A*.

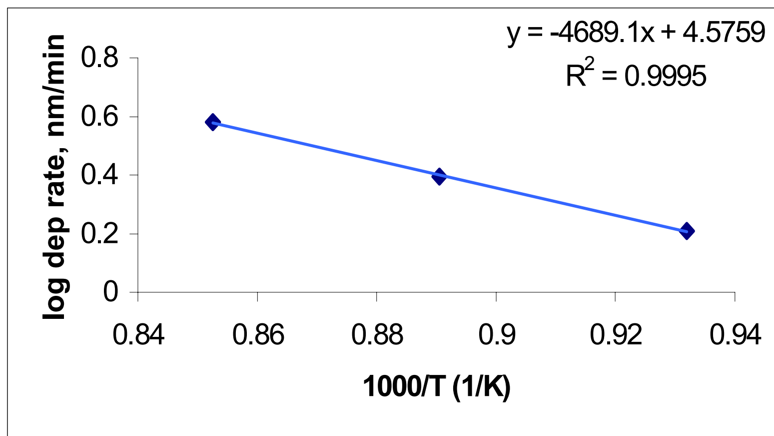

Figure 11 Arrhenius' plot.(Note that in regression equation, x = 1/T).

The activation energy obtained from this experiment was 21.454 kcal/mol. This value is comparable to the activation energy for a SiH_4-NH_3-N_2 LPCVD system reported elsewhere[14], which is 20 kcal/mole. Since the activation energy is higher than 10 kcal/mol, we can conclude that *surface reaction* is rate limiting[15]. The Arrhenius' constant obtained was 37661.7. Therefore, the rate equation obtained from this experiment was:

$$\textbf{Deposition rate, nm/min} = 37661.7 \exp(-4689.1/T) \quad (5)$$

4.3 Results of the Scanning Electron Microscopy

Examination of the photomicrographs shown in Figure 12 reveals a deposit composed of spherical-cap shaped clusters of silicon nitride with a maximum diameter of approximately 0.38 micron when viewed perpendicular to the wafer surface (Fig. 12a). The clusters grew preferentially along unconstrained directions and were deformed to a polygon as their boundaries meet. These boundaries constrain the growth of the clusters. Viewing with the wafer inclined at an angle of 54° with respect to the sample stage (Fig.12b) reveals a rough film surface. Clusters found on top were larger because their growth was less constrained, while those at the bottom were smaller because of the presence of neighboring clusters. The deposition was not planar, i.e. some clusters start to form on top of other clusters even though the previous layers were not yet completely filled.

A cut of about 25μm x 30μm x 3μm was made on the wafer surface using a focused ion beam (FIB). The cut surface was observed using SEM at a tilt angle of 54° (Fig. 13). The first layers of silicon nitride covering the silicon wafer have a relatively smooth surface. On top of this layer, we can see spherical-cap shaped silicon nitride clusters of varying sizes, which render the film surface rough. A possible explanation for this change in morphology is that initially the nucleation rate is faster than the growth rate. This results to the formation of many small nuclei and thus producing a smoother surface. As the film thickens, the growth rate becomes faster than the nucleation rate. Fewer nuclei are formed but these nuclei are able to grow into larger clusters. Due to the roughness of the film, thickness measurement using SEM is quite difficult. Averaging the film thickness, however, would give us roughly the same value as that of the ellipsometer reading, which is about 0.18 micron (180 nm).

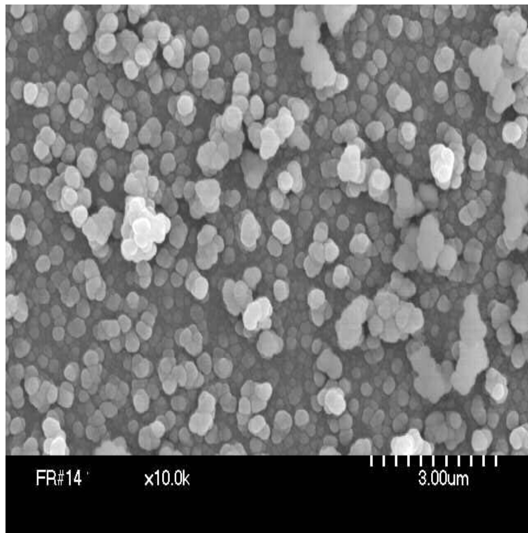

(a)

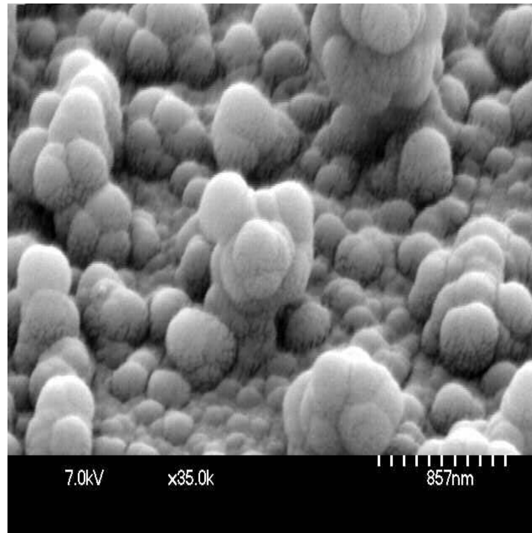

(b)

Fig 12 SEM photomicrograph the specimen deposited at T=900°C, p=4torr, R=99, and t=60mins. (a) tilt = 0° (b) tilt = 54°

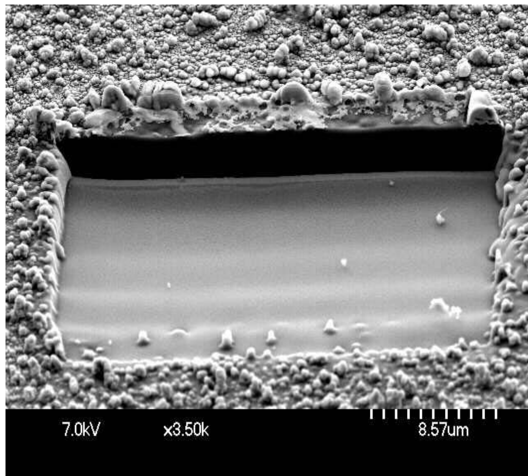

(a)

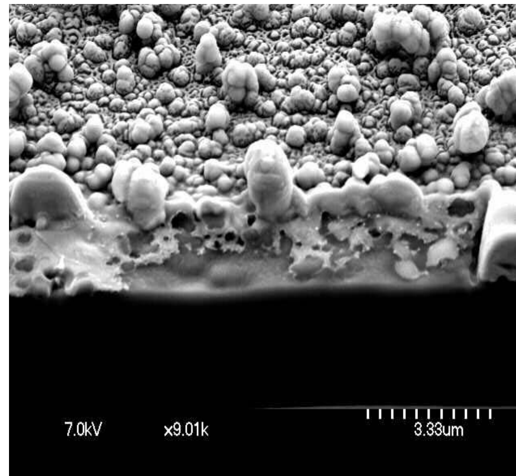

(b)

Figure 13 FIB cut on the control specimen. Specimen tilt = 54°. (a) lower mag. (b) higher mag.

4.5 Energy Dispersive X-ray (EDX) Analysis Result

The result of the energy dispersive X-ray (EDX) analysis is given in Figure 14. The silicon nitride layer was deposited at 850°C for 40 minutes with an NH_3/SiH_4 ratio of 66 and a pressure of 5 torr. The average thickness of the deposited layer is 140 nm. Both nitrogen and oxygen were detected together with silicon. The aluminum peak can be attributed to the sample holder. The nitrogen peak suggests the formation of silicon nitride. Oxygen in the film can be attributed to the SiO_2 layer produced by the chemical cleaning prior to silicon nitride deposition. It has been observed that silicon nitride deposited by LPCVD on silicon, exhibits a 15 to 20% SiO_2 layer between silicon and silicon nitride[16]. Complete removal of this extraneous oxide layer can be achieved using *in situ* HF vapor cleaning[17].

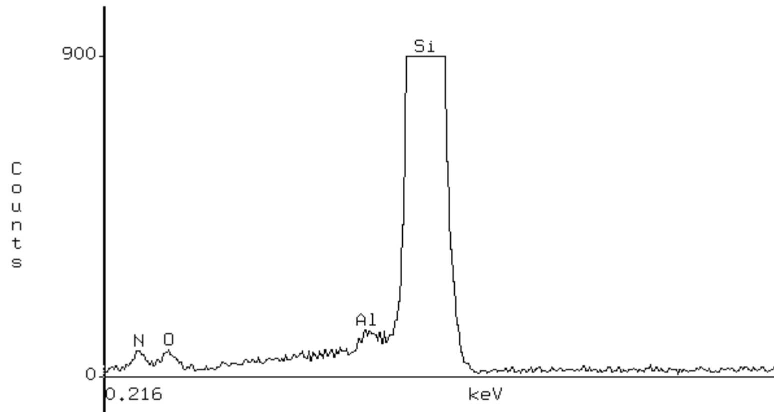

Figure 14 Energy dispersive X-ray (EDX) result of the deposited film.

4.6 Result of X-ray Diffraction Analysis

No peaks were obtained for the as-deposited sample which means that the deposit is amorphous. This agrees with the expected structure. The x-ray diffraction pattern of the silicon nitride deposit on the quartz glass wafer holder after annealing in air at 1400°C for 4 hrs is shown in Figure 15. After the annealing treatment, peaks of SiO_2 and α-Si_3N_4 were obtained. From these results, we can conclude that the amorphous deposit produced by LPCVD using silane and ammonia gases was silicon nitride since crystalline α-Si_3N_4 was obtained after the annealing treatment. SiO_2 peaks were present because of oxidation of the silicon nitride film during high temperature annealing in air. Annealing in vacuum would prevent film oxidation.

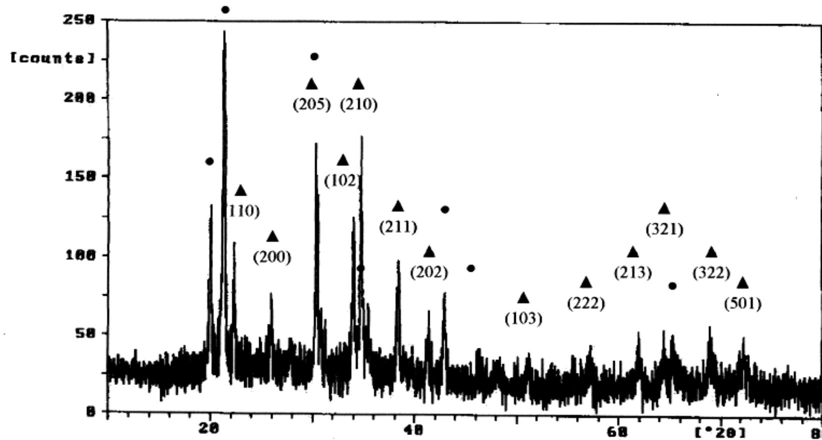

Figure 15 X-ray diffraction pattern of the silicon nitride deposit on the glass wafer holder after annealing in air for 4 hrs. at 1400°C.
● - SiO_2 , ▲- Si_3N_4

IV. Conclusions

The effects of the deposition parameters on the thickness of the silicon nitride film deposited by LPCVD method were investigated in this study. The film thickness was found to increase with an increase in temperature (A), pressure(B) and time(D), and a decrease in NH_3/SiH_4 flowrate ratio(C). All main effects and interactions AC, AD, and CD were statistically significant. A first order interactive model based on the results of the factorial study was obtained. The computed activation energy of 21.454 kcal/mol indicates that surface reaction is rate limiting. The deposited film has a rough morphology composed of spherical-cap shaped clusters of silicon nitride. EDX and XRD analyses confirm the formation of silicon nitride.

V. Acknowledgements

The author would like to acknowledge the DOST-PCASTRD for the financial support of this study as part of the project “Development of Patterning and Layering Procedures for Semiconductor Device Fabrication”. I also wish to acknowledge the following: Dr. Alberto A. Amorsolo, Jr. and Dr. Meliton U. Ordillas, Jr. for the technical guidance; and Engr. Paul C. Concepcion for the SEM micrographs.

References

1. M. Yoshimaru, et. al., *Effects of Deposition Temperature on the Oxidation Resistance and Electrical Characteristics of Silicon Nitride*, IEEE Transactions on Electron Devices, Vol.41, No.10, (October 1994).
2. T. Klein et al., *Silicon Nitride PECVD at Low Temperature: film Properties and Plasma Analysis*.
3. H. Amjadi and G.M. Sessler, *Charge storage in APCVD Silicon Nitride,* IEEE Annual Report-Conference on Electrical Insulation and Dielectric Phenomena, Minneapolis (Oct 19-22, 1997).
4. G. Roman, *Process Characterization of LPCVD Silicon Nitride and the Consequential Fabrication of Low Stress Microcantilevers*, National Nanofarication Users Network.
5. T.P. Ma*, Making Silicon Nitride Film a Viable Gate Dielectric*, IEEE Transactions on Electron Devices, Vol. 45, No.3, (March 1998).
6. K. Nybergh, *Modeling the growth of PECVD Silicon Nitride Films for Crystalline Silicon Solar Cells using Factorial Design and Response Surface Methodology,* IEEE, 26th PVSC, Anaheim, Ca. (Sept.30-Oct.3,1997)
7. S. Sivaram, “Chemical Vapor Deposition, Thermal and Plasma Deposition of Electronic Materials”, Van Nostrand Reinhold, p.1, (1995).
8. C.Y. Chang and S.M. Sze, “ULSI Technology”, McGraw-Hill, p. 211, (1996).
9. A. Sherman, “Chemical Vapor Deposition For Microelectronics”, p.37, (1987).
10. Belyi et al., “Silicon Nitride in Electronics”, Elsevier, pp. 52-53, (1988).
11. R. Hamilton, *NanoSpec Manual*, EECS 143 Microfabrication Technology, http://snf.stanford.edu/.edu, (1996).
12. D.J De Smet, *Description of an Ellipsometer*, http://www.uronramp.net /~ddesmet/bk/part1/part1a.html, (1995).
13. A. Amorsolo, *Manual on the Methodology Behind the Design and Analysis of Multifactor Experiments*, p. 99, (1998).
14. Morosanu, “Thin Films by Chemical Vapor Deposition”, Elsevier, pp.138-140, (1990).
15. H. Alan Fine, *Extractive Metallurgy Laboratory Exercises*, The Metallurgical Society of AIME, NY, p. 116, (1982).
16. Arthur Sherman, “Chemical Vapor for Microelectronics: Principles, Technology, and Applications”, Noyes Publications, p. 77, (1987).
17. M. Ino et al., *Silicon Nitride Thin-Film Deposition by LPCVD with In Situ HF Vapor Cleaning and Its Application to stacked DRAM Capacitor Fabrication*, IEEE Transactions on Electron Devices, Vol. 41, No.5, (May 1994).

APPENDIX

Yate's technique for computing contrast

Treat. Comb.	*Response (nm)*	*1*	*2*	*3*	*4*	*Comment*
1	56.56	207	496.5	706.92	2604.96	Total sum of responses
a	150.44	289.5	210.42	1898.04	1126.16	a contast
B	86.32	82.08	1337.48	296.28	429.72	b contrast
ab	203.18	128.34	560.56	829.88	100.12	ab contrast
c	19.32	561.72	210.74	128.76	-1063	c contrast
ac	62.76	775.76	85.54	300.96	-468.84	ac contast
bc	43.12	236.82	586.76	21.64	-163.36	bc contrast
abc	85.22	323.74	243.12	78.48	-111.84	abc contrast
d	154.92	93.88	82.5	-286.08	1191.12	d contrast
ad	406.8	116.86	46.26	-776.92	533.6	ad contrast
bd	220.44	43.44	214.04	-125.2	172.2	bd contrast
abd	555.32	42.1	86.92	-343.64	56.84	abd contrast
cd	56.5	251.88	22.98	-36.24	-490.84	cd contrast
acd	180.32	334.88	-1.34	-127.12	-218.44	acd contrast
bcd	102.22	123.82	83	-24.32	-90.88	bcd contrast
abcd	221.52	119.3	-4.52	-87.52	-63.2	abcd contrast

Effect = (2 x contrast) / 16